IOWA STATE UNIVERSITY
Digital Repository

9-1981

Advances in Computer Reconstruction of Acoustical Holography

V. Schmitz
Fraunhofer Institut für zerstörungsfreire Prüfverfahren

R. Kiefer
Fraunhofer Institut für zerstörungsfreire Prüfverfahren

G. Schäfer
Fraunhofer Institut für zerstörungsfreire Prüfverfahren

Recommended Citation

Advances in Computer Reconstruction of Acoustical Holography

Abstract

The article describes the results of two methods: the Fresnel approximation and the convolution method used for the exact Rayleigh-Sommerfeld equation. Curves for the Fresnel approximation are shown as a function of flaw depth and number of sample points. Despite a violation of the fresnel condition, an image can be achieved without visible phase distortion. This and its limits are shown on synthetic and experimental data. By shifting the hologram and not changing the symmetric phase factor, calculation time is saved because the rearrangement in the image space is achieved automatically. The exact method "angular spectrum" has been simplified in three steps. For different insonification angles in shear wave holography, the data set must be multiplied by an aperture function before being Fourier transformed. Examples demonstrate the usefulness of contact technique probes. To improve the recording time, a 140 element array will be multiplexed electronically and moved mechanically.

Keywords
Nondestructive Evaluation

Disciplines
Materials Science and Engineering

ADVANCES IN COMPUTER RECONSTRUCTION
OF ACOUSTICAL HOLOGRAPHY

V. Schmitz, R. Kiefer, G. Schäfer
Fraunhofer Institute für zerstörungsfreie Prüfverfahren
Saarbrücken, West Germany

ABSTRACT

The article describes the results of two methods: the Fresnel approximation and the convolution method used for the exact Rayleigh-Sommerfeld equation. Curves for the Fresnel approximation are shown as a function of flaw depth and number of sample points. Despite a violation of the fresnel condition, an image can be achieved without visible phase distortion. This and its limits are shown on synthetic and experimental data. By shifting the hologram and not changing the symmetric phase factor, calculation time is saved because the rearrangement in the image space is achieved automatically. The exact method "angular spectrum" has been simplified in three steps. For different insonification angles in shear wave holography, the data set must be multiplied by an aperture function before being Fourier transformed. Examples demonstrate the usefulness of contact technique probes. To improve the recording time, a 140 element array will be multiplexed electronically and moved mechanically.

INTRODUCTION

Image formation in holography can be achieved optically and numerically (Ref. 1). The numerical reconstruction has several advantages versus optical reconstruction: objectivity, reproducibility and free scaling image enhancement. Some shortcomings are: high costs and long reconstruction time with conventional data processing. We will describe here basic developments in performing the calculations on a PDP 11/34 computer, our experiences with the implementation of the Fresnel approximation and the angular spectrum method and show the direction for implementing a fast recording and reconstruction system.

FRESNEL RECONSTRUCTION

A measure for the quality of an acoustic image is the resolution achieved in the image space. In addition, the effect of phase errors introduced by the paraxial approximation or by the expansion of the phase factor have to be carefully investigated. Figure 1 shows a two-dimensional Fresnel reconstruction of flat bottom holes at a depth of 100 mm in steel. The pattern in the center consists of 3 mm holes with edge-to-edge separations down to 1 mm, corresponding to 2.2 wavelengths at 2.66 MHz frequency. A resolution of better than 2 mm at this great depth could easily be achieved. The outer circle demonstrates the sensitivity for the Fresnel reconstruction. The smallest dot corresponds to a 3 mm hole, the largest one to a 10 mm hole.

To investigate the effect of different degrees of violation of the Fresnel conditions I and II (Fig. 2), we used synthetic data and varied the flaw depths z between 60 mm and 200 mm and increased finally the frequency, so that the ultrasonic wavelength decreased from 3 mm to 0.5 mm. Figure 2 shows the phase disturbances when the flaw depth varies. In case No. 1, despite "8" being less than "156", the reconstruction is correct. In cases No. 2 to 6, the error in the square root expansion gets more and more severe and results finally in severe phase distortions. To get a more quantitative description, Fig. 3 shows the Fresnel conditions for three different longitudinal and shear wave wavelengths. If the actual data lie
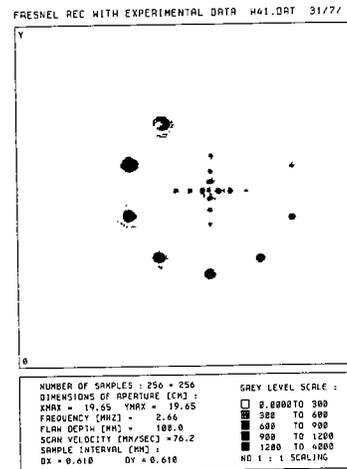

FRESNEL REC WITH EXPERIMENTAL DATA H41.DAT 31/7/

NUMBER OF SAMPLES : 256 x 256
DIMENSIONS OF APERTURE [CM] :
XMAX - 19.65 YMAX - 19.65
FREQUENCY [MHZ] - 2.66
FLAW DEPTH [MM] - 100.0
SCAN VELOCITY [MM/SEC] -76.2
SAMPLE INTERVAL [MM] :
DX - 0.610 DY - 0.610

GREY LEVEL SCALE :
☐ 0.000 TO 300
▨ 300 TO 600
▩ 600 TO 900
■ 900 TO 1200
■ 1200 TO 4000
NO 1 : 1 SCALING

Fig. 1 Fresnel reconstruction, 256 x 256 samples, flaw depth - 100 mm; frequency - 2.6 MHz.

Fresnel-conditions:

I: $z > L_F + L_H$

II: $z^3 > \frac{\pi}{4 \cdot \lambda}(L_F + L_H)^4$

$\Delta x_B = \frac{\lambda \cdot z}{N \cdot \Delta x}$
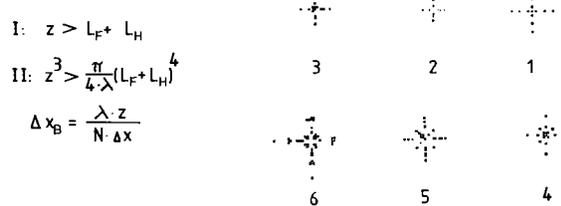
No.	z mm	λ mm	$L_F + L_H$ mm	$z^3 \cdot 10^6$	Right Side II.	I.	II.
1	200	0.5	100	8	156	Yes	No
2	200	3	102	8	28	Yes	No
3	150	3	100	2.2	26	Yes	No
4	120	3	100	1.4	26	Yes	No
5	100	3	97	1.0	23	No	No
6	60	3	101	0.2	27	No	No

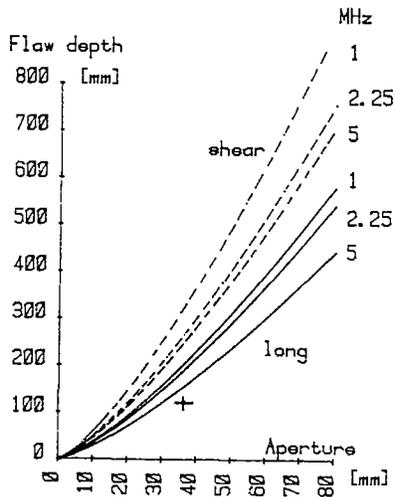Fig. 2 Effect of Violation of the Fresnel conditions.

203

Fig. 3 Validity of Fresnel approximation: region above the curves.

above the curve, the phase distortions can be neglected. If they lie below the curve, there is a large possibility that the result will be correct. This demonstrates clearly that the Fresnel conditions are only a sufficient criterion. Figure 4 shows a correct reconstruction of a Y-shaped flaw in 120 mm depth, where the Fresnel approximation, marked by "+", is slightly violated. The image resolution is about 1.4 mm.
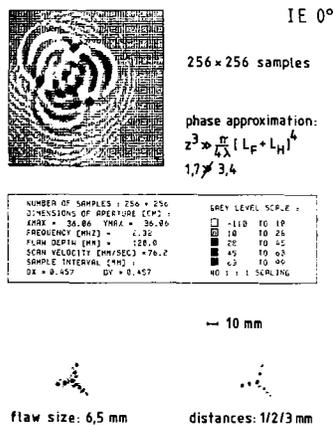

Fig. 4 Fresnel reconstruction with an experimental data set.

In Fresnel reconstruction, the holographic data are multiplied by an exponential function and then Fourier transformed. The integral has to be converted to a discrete Fourier series in order to calculate the FFT in the computer. The substitution, $x' - L_H = x''$, shifts the aperture L_H into the positive domain and the quadratic phase factor is shifted too. To get a nondistorted picture in the image space, we have to exchange the data set $(0, \pi/T)$ with the data set $(\pi T, 2\pi/T)$. This requires additional calculation time. If we shift the hologram by L_H and do not change the symmetric

phase factor (Ref. 2), this is done automatically. One additional effect is the shift of the image by the amount of $2 L_H/\lambda z_{12}$ (Fig. 5).

$$|u_2(\bar{x})|^2 = \left|\int_0^{2L} u_1(x'-L) \cdot \exp[-\frac{i\pi}{\lambda z}(x'^2 - 2\bar{x}x')] \, dx'\right|^2$$

$$|u_2(\bar{x})|^2 = \left|\int_0^{2L} u_1(x'-L) \cdot \exp[-\frac{i\pi}{\lambda z}(x'^2 - 2x'(\bar{x}+L))] \, dx'\right|^2$$
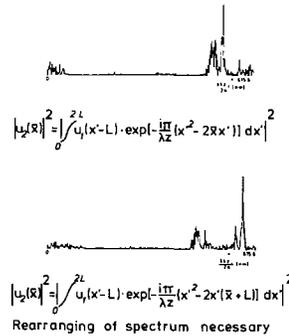
Rearranging of spectrum necessary

Fig. 5 Fresnel reconstruction with symmetric and asymmetric phase factor.

ANGULAR SPECTRUM METHOD

The interpretation of the Rayleigh-Sommerfeld equation in the form of a convolution leads to an exact solution. But instead of one fast Fourier transformation, we have to perform three FFT's. We will show now that it is possible to use fewer sample points and to decrease the calculation time. The improvement is shown with the aid of a data set of 128 x 128 sample points and longitudinal waves. In the last step, this method is adapted to 45° shear waves.

Figure 6 shows the reconstruction with the angular spectrum method by a computer simulation. At the top, the real part and imaginary part of the exponential function can be seen; in the middle, the real part and the imaginary part of the synthesized holographic data are seen and at the bottom, the intensity distribution in the image space, which reproduces the image of point-like flaws with edge-to-edge separation of 1 mm to 6 mm can be seen.
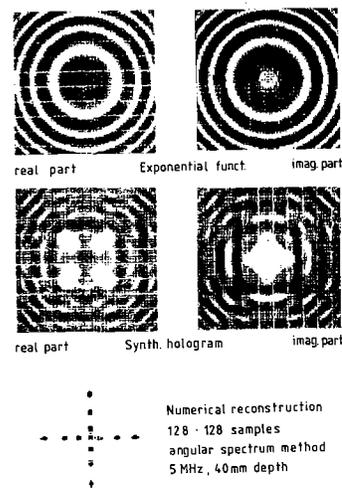

Fig. 6 Angular Spectrum Method with synthetic holographic data set.

For the development of the convolution, we used experimental values of flaws at a depth of 120 mm, with an ultrasonic frequency of 2.32 MHz. The conventional use of the convolution needs a "fill up" by zeros, so if the data set is limited to 128 x 128, only 64 x 64 data can be used for experimental data. This restricts the aperture. Figure 7 shows the data set together with the exponential function and its Fourier transform. Because the exponential function has to be truncated very early, its amplitude has not yet diminished sufficiently. This causes ripples in the Fourier domain and hence phase distortions in the image domain. Nevertheless, the image reconstruction in the figure below agrees very well with the flat bottom holes.

CONVOLUTION

64 x 64 samples
holographic data
imaginary part

exp-function and "0"
128 x 128

fourier transformation

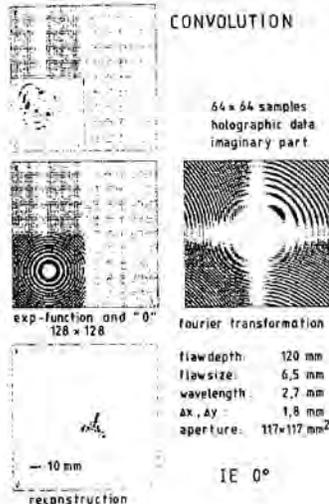| flaw depth: | 120 mm |
flaw size:	6.5 mm
wavelength:	2.7 mm
Δx, Δy :	1.8 mm
aperture:	117×117 mm²

— 10 mm

reconstruction

IE 0°

Fig. 7 Angular Spectrum Method filled up by zeroes computer FFT of the exponential function.

This phase error can be avoided by using the Fourier transform of the exponential function taken from -infinity to +infinity. The analytically transformed function extends from $-\infty$ to $+\infty$ too. This function is now shifted in such a manner that the low frequencies lie in the lower left corner. Then this data set is mirrored into the other three quadrants. After multiplication, with the transformed data set, the inverse transform produces the image shown at the bottom of Fig. 8. A comparison in the frequency content of the hologram at the top and the propagation function in the middle shows that only three fringes of the propagation function contribute to the image. Higher frequencies are eliminated by the evanescing hologram transform amplitudes. The sample rate can now be adapted to the highest frequency content of the experimental data and not to the highest frequency of the propagation function in the middle of its aperture. This results in an increase in the investigated material volume, while keeping the computer calculation time and computer memory size constant.

The mirroring of the transformed propagation function into the other three quadrants is the prerequisite for the last step of the development, the use of 128 x 128 experimental values instead of 64 x 64 and adding zeroes to fill up the 128 x 128 data. The software for performing these calculations will run within 40 minutes on a PDP11/50

CONVOLUTION

64 x 64 samples
filled up with " 0"
to 128×128

FFT of holographic data

direct fourier transf.
of the transfer function
for 64 × 64 samples
folded symmetrically
to 128 × 128 data

IE 0°
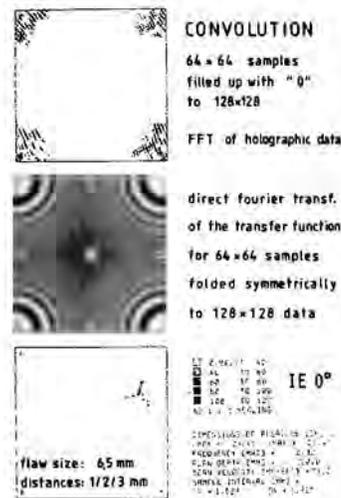
flaw size: 6.5 mm
distances: 1/2/3 mm

Fig. 8 Angular Spectrum Method, filled up by zeroes, direct calculation of the exponential function and its mirror pictures in the frequency domain.

computer or within five minutes on a VAX. The results are shown in Fig. 9, with two different grey level scales and shows an excellent agreement with the true flaw dimensions.

CONVOLUTION

128 × 128 samples

IE 0°

direct fourier transf.
of the transfer function
for 64 × 64 samples
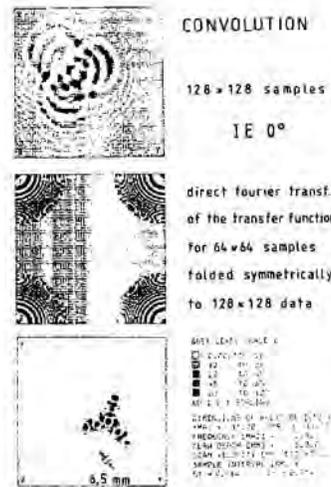folded symmetrically
to 128 × 128 data

6.5 mm

Fig. 9 Angular Spectrum Method; use of the entire field for experimental data, direct calculation of the exponential function and its mirror pictures in the frequency domain.

In the above examples, we used vertical insonification with longitudinal waves. In the case of shear waves, the sound beam modulates the holographic data $V(x,y)$. This means the spectrum is shifted to higher frequencies. By introducing an aperture function, $b(x,y)$, the spectrum can be shifted back. The formalism for pulse echo with longitudinal, or with shear waves under arbitrary angles in x direction, is given by the following equation:

$$|u(x,y)|^2 = |F^-\{F^+[b(x.y)V(x,y)] \cdot \tag{1}$$

$$\exp. [ikz\sqrt{1-\lambda^2(\zeta^2 + \eta^2)}]\}|^2$$

with

$$b(x,y) = \exp.(i\frac{2\pi}{\lambda} x \sin\alpha) \tag{2}$$

In the case of pulse echo 0°, we have $\alpha = 0°$ and $b(x,0) = 1$.

This illumination function, $b(x,y)$, has to be used only in the angular spectrum method. According to the shift theorem, it would only shift the image in the Fresnel approximation formalism. Fig. 10 shows the effect of the illumination function for a 45° shear wave. The information in the frequency domain on the right-hand side is shifted to the lower frequency domain and can now be multiplied by the propagation function to perform the necessary steps for the final Fourier back transformation.

Fouriertransformed: holographic data
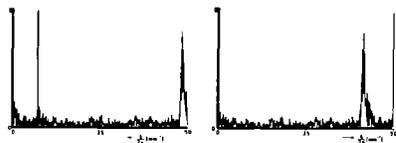
45° illuminating
function shifts the
spectrum back

vertical illuminating
function

Fig. 10 Effect of the illumination function to correct the modulation by the shear wave insonification.

INSTRUMENTATION

The above formalism has been implemented on a PDP 11/34 computer. To improve the reconstruction time, a MAP 300 array processor will reduce the time between data recording and image presentation to about 60 seconds for a set of 128 x 128 sample points. Until now, a two dimensional scanner moved the probe in a square wave scan pattern. The scan time needed was about 180 seconds. This time can be reduced to about 56 seconds by the application of the electronic scheme shown in Fig. 11. Measurements of the sound field of an 140 element linear 2 MHz array showed amplitude variations of less than 1 dB. These elements will be multiplexed electronically, but eight elements will be switched together to obtain a sufficient signal/noise ratio.

Besides the data recording and reconstructing time, an easy to handle probe and probe holding device are very important. Figure 12 shows a 45°, 2.25 MHz probe in the contact technique with a water gap of about 1/2 mm. The probe is spring loaded against the wall and can follow its curvature. The same technique will be applied to the large 140 mm array or smaller arrays.

CONCLUSIONS

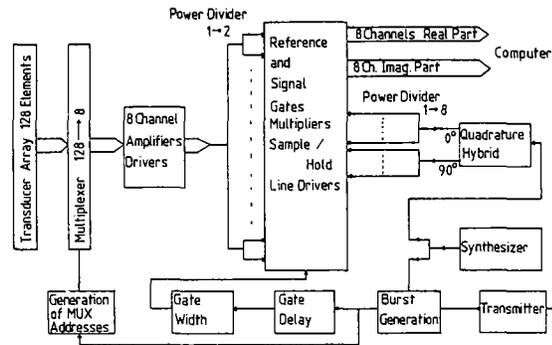It has been shown that the resolution limit for shear or longitudinal waves is one wavelength

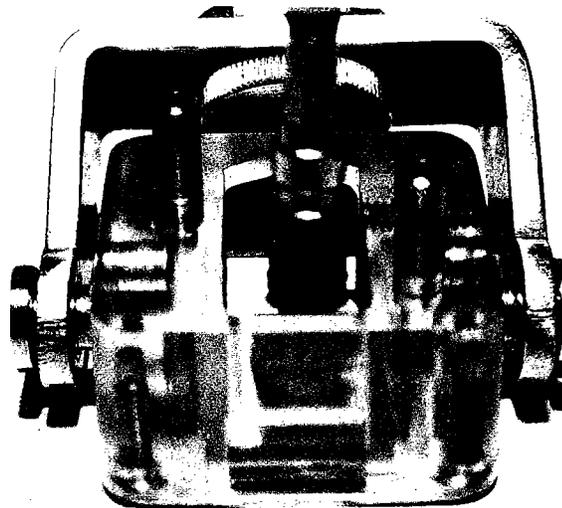Fig. 11 Quasi-realtime holography.

Fig. 12 2.25 Mhz shear wave probe in contact technique for holography.

and it could be achieved by both Fresnel reconstruction, as well as the exact angular spectrum method. Phase errors will cause artifacts if the Fresnel conditions are strongly violated. In most practial cases, as shown by comptuer simulation and corresponding experiments, small violations of the Fesnel condition are tolerable. A technique has been presented where time can be saved in calculating the Fresnel reconstruction because the rearranging in the spectrum is done automatically. Time and computer storage capacity has been saved in the angular spectrum method by calculating a shifted propagation function in the Fourier domain and mirroring it into the remaining three quadrants. In the case of shear waves, the sound beam modulates the holographic data. By multiplying the experimental data by an aperture function, a distortion-free holographic image is calculated. These formalisms have been implemented on a PDP 11/34 computer. Current work is directed towards reducing the data collecting time by multiplying a 140 element linear array.

206

ACKNOWLEDGMENTS

REFERENCES

1. V. Schmitz, and M. Wosnitza, "Experiences Using Ultrasonic Holography in Laboratory and in the Field with Optical and Numerical Reconstruction", Acoustic Imaging, Vol. 8, Metherell Plenum Publishing Corp., pp. 651-683.

2. K.J. Langenberg, R. Kiefer, M. Wosnitza and V. Schmitz, "Zur Numerischen Rekonstruktion von Ultraschall - Hologrammen," Intern. Symp. "New Methods of Nondestructive Testing of Materials and Their Application Especially in the Nuclear Industry", Saarbrücken, West Germany, September 17-19, 1979.